Thin Solid Films 517 (2009) 2353–2356

Contents lists available at ScienceDirect

Thin Solid Films

journal homepage: www.elsevier.com/locate/tsf

Analysis of electrical properties of CIGSSe and Cd-free buffer CIGSSe solar cells

J. Marlein *, K. Decock, M. Burgelman [1]

Gent University, Electronics and Information Systems (ELIS), St-Pietersnieuwstraat 41, B-9000 Gent (B), Belgium

ARTICLE INFO

Available online 13 November 2008

Keywords:
Solar cell
CIGS
Electrical properties
Buffer layers
In_2S_3
ZnMgO

ABSTRACT

We investigated the influence of different buffer layers to the electrical parameters (J_{sc}, V_{oc}, *QE* and efficiency η) of solar cells. The cells with an In_2S_3 and a ZnMgO buffer layer were compared with a reference cell with a CdS buffer layer. We performed temperature and light dependent current-voltage measurements, temperature dependent capacitance measurements and quantum efficiency measurements.
The cells with In_2S_3 and ZnMgO buffers differ not too much in J_{sc}, but they do differ in V_{oc} and their electrical properties — fill factor *FF*, diode saturation current J_0 and efficiency η. They also do differ in their spectral response, both at short and long wavelengths, and in their ideality factor. This indicates a different current transport mechanism. The device simulation program SCAPS is used for further interpretation of the measurements. After exploring the parameters we found an acceptable agreement between simulated and measured *J–V* and *QE*(λ) curves. The simulated *QE* curves fit well over the whole spectrum, except for the CdS buffer cell, where there is an overestimation for the intermediate wavelengths. Because of this the simulated J_{sc} is higher than the measured one. The simulated V_{oc} agrees well for all cells. For the ZnMgO buffer cell it was necessary to include a buried homo-junction.

1. Introduction

Thin film solar cells based on chalcopyrite semiconductors have reached a high level of performance over the last years both for laboratory scale cells and commercial products [1]. Polycrystalline thin-film $CuIn_{1-x}Ga_xSe_2$-based (CIGS) solar cells have recently achieved 19.9% efficiency [2]. The cell used a traditional *p*/*n* junction with a layered cell structure glass/Mo/CIGS/CdS/ZnO. In all very high efficiency CIGS cells, the buffer layer is a CdS layer deposited by CBD (Chemical Bath Deposition). Many efforts are going on to replace this buffer layer by more attractive alternatives. Ideally the buffer layer should (i) be an *n*-type material with a wider energy gap than CdS (thus $E_g > 2.42$ eV) and with a good match to CIGS (both lattice and band alignment), (ii) be deposited by vacuum techniques which are more in line with the techniques for the other layers, thus avoiding the wet chemistry step of CBD, and (iii) avoid any chemicals which could cause problems with public acceptance, like Cd. Many alternative buffer materials have been tested out [3,4], and though none of them has yet beaten the performance of a CIGS cell with a CdS CBD buffer layer, some 'alternative buffers' are performing very well.

In this article we will discuss electrical measurements and simulations on chalcopyrite solar cells with two alternative buffer layers — In_2S_3 and ZnMgO, and compare them with CIGS cells with a CdS CBD 'reference buffer'.

2. Experimental details

The samples used were prepared at AVANCIS (Germany). The key features of the process are: controlled sodium doping, deposition of a Cu–In–Ga–Se elemental precursor stack, rapid thermal processing (RTP) in a sulphur-containing ambient, sputtering deposition of a ZnO window layer [1,5–7]. Because of the sulphur addition to the CIGS surface in the RTP process step, we call this absorber material Cu(In,Ga)(S,Se) or CIGSSe. Current–voltage *J–V* and J_{sc}–V_{oc} measurements are performed with a four-point probe technique and a Source Measure Unit 236 Keithly. For the illuminated *J–V* measurement we used an Oriel 81160 solar simulator with an uniform light spot of 5×5 cm^2 and with AM1.5G spectral filters. For the J_{sc} –V_{oc} measurements we used an Oriel 6143 lamp together with neutral density filters, to achieve 16 different illumination levels, ranging from about 1 to 1500 W/m^2. External quantum efficiency *QE* measurements were carried out in the 300–1400 nm wavelength range, in dark, and without voltage bias. The measurements shown below are typical for the buffer/absorber combination in this study.

3. Results and discussion

3.1. Current–voltage measurements

In Fig. 1 the *J–V* curves of a typical cell in light and dark are plotted. In Table 1 the main photovoltaic parameters J_{sc}, V_{oc}, *FF* and η deduced from these *J–V* curves are summarised. These were measured in AVANCIS, and the active cell area was used for determination of J_{sc} and η. The measured *J–V* curves of the three cells have a comparable shape. The cells with the

* Corresponding author. Tel.: +32 9 264 8953.
E-mail address: Jonas.Marlein@elis.ugent.be (J. Marlein).
[1] Tel.: +32 9 264 3381.

0040-6090/$ – see front matter © 2008 Elsevier B.V. All rights reserved.
doi:10.1016/j.tsf.2008.11.048

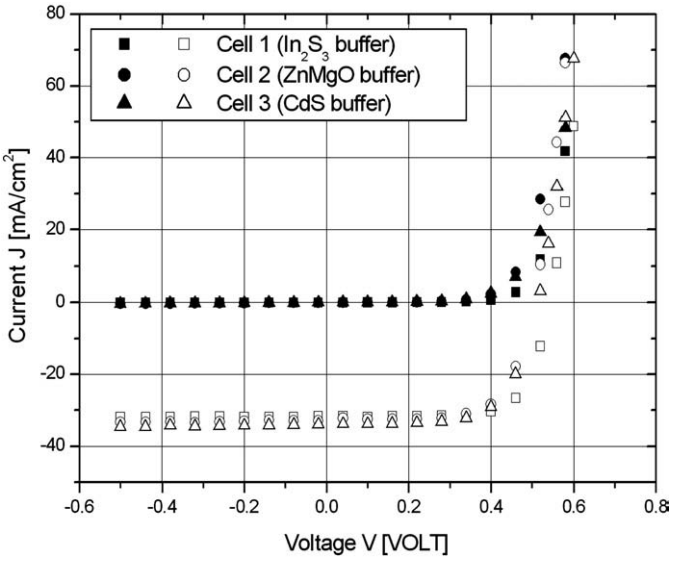

Fig. 1. Dark and light curves of a typical cell. Cell 1 has an In_2S_3 buffer layer, cell 2 - a ZnMgO buffer and cell 3 - a CdS buffer.

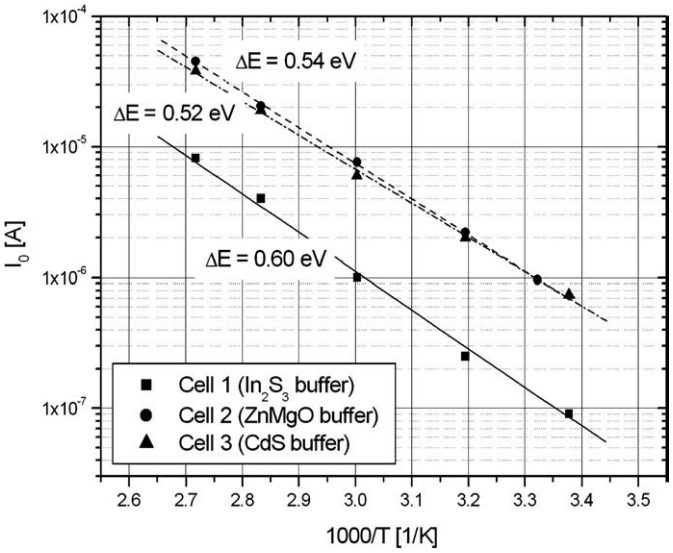

Fig. 2. Saturation current vs. 1/*T*. Squares: In_2S_3 buffer; circles: ZnMgO buffer; and triangles: CdS buffer.

CdS reference buffer and with the ZnMgO buffer have comparable performance parameters; compared to them, the cell with the In_2S_3 buffer has a higher V_{oc}, but also a lower J_{sc}. All three cells show a crossover of the light and dark *J*–*V* curves.

We have used an empirical method [8,9] to study the non-idealities. We conclude that shunt conductance G_{sh} is dominant non-ideality. The values of G_{sh} and the diode non-ideality factor *n* are also listed in Table 1.

3.2. Saturation current

Temperature dependent dark current voltage measurements were carried out to find the dominant current transport mechanism, following standard procedures outlined, e.g., in [10]. If the current is limited by recombination in the absorber quasi-neutral region, then the saturation current is modelled by the ideal Shockley theory, the diode ideality factor is unity ($n=1$), and the saturation current is thermally activated with the band gap energy E_g.:

$$J_0 \propto \exp\left(-\frac{E_g}{kT}\right). \quad (1)$$

If the main current mechanism is recombination in the space charge layer, then $n=2$, and the diode saturation current is activated with a lower activation energy, which is half the band gap energy when recombination is through the mid gap states:

$$J_0 \propto \exp\left(-\frac{E_g}{2kT}\right). \quad (2)$$

If both mechanisms are present, the current depends exponentially on voltage, which is in a (possibly limited) voltage range described by an ideality factor $1<n<2$ and a thermally activated saturation current $J_0 \propto \exp\left(-\frac{\Delta E}{nkT}\right)$, with the activation energy ΔE in the range $E_g/2<\Delta E<E_g$. The parameters *n* and J_0 are determined from the temperature dependent log(*J*) vs. *V* plots, and ΔE is then derived from the Arrhenius plot of J_0. Such Arrhenius plots for cells with the three buffer layers are shown in Fig. 2.

The activation energies ΔE derived from these Arrhenius plots are also listed in Table 1. The band gap of the measured CIGS material is approximately 1 eV (Table 2). The values we find are thus about half of the band gap of the absorber, we conclude that recombination in the space charge region is the dominant current mechanism. Other possible mechanisms, such as interface recombination or tunnelling do not seem to play a determining role here [10].

Table 1
Cell parameters under AM1.5 illumination

Cell		1	2	3
Buffer layer		In_2S_3	ZnMgO	CdS
J_{sc}	mA/cm²	32.6	34.0	35.2
V_{oc}	mV	557	515	564
FF	%	72.4	69.0	69.8
η	%	13.33	12.09	13.87
n		1.68	1.82	1.98
G_{sh}	mS/cm²	0.9	1.1	0.8
ΔE	eV	0.60	0.54	0.52

3.3. Capacitance measurements

The *C*(*f*,*T*) measurements of cell 2 (ZnMgO buffer) in the temperature range 299 K–368 K are plotted in Fig. 3.

The resonance peak seen at 1 MHz is not a feature of the CIGSSe solar cell, but is caused by resonance with the inductance *L* of the leads and the internal circuitry of the measurement equipment. Assuming a value of $L=0.5$ μH, we could quantitatively explain both the position and the shape of the measured *C*–*f* curves [11]. In all interpretations we thus limit the discussions to lower frequencies $f<200$ kHz.

The capacitance slowly decays over a broad frequency range 100 Hz–100 kHz. This hints to a defect band distributed over a broad range in the

Table 2
Main simulation parameters of the different cells. The charge type of the doping, the defects and the interface states is also indicated with A (acceptor) of D (donor)

Parameter		In_2S_3	ZnMgO	CdS
Absorber				
Thickness	μm	1.5	1.5	1.5
Thickness *n*-layer	μm		0.1	
Band gap	eV	1.01	1.01	1.01
Doping density (A)	cm^{-3}	$7.0\ 10^{15}$	$1.0\ 10^{16}$	$2.4\ 10^{16}$
Defect density (D)	cm^{-3}	$3{\cdot}10^{14}$	$7{\cdot}10^{14}$	$4{\cdot}10^{15}$
Interface				
Density of states (D)	cm^{-2}	$1{\cdot}10^{10}$	$1{\cdot}10^{11}$	$2{\cdot}10^{12}$
Buffer				
Thickness	μm	0.06	0.06	0.06
Band gap	eV	2.50	3.47	2.50
Doping density (D)	cm^{-3}	$5{\cdot}10^{17}$	$5{\cdot}10^{17}$	$5{\cdot}10^{17}$
Defect density (A)	cm^{-3}	$1{\cdot}10^{17}$	$1{\cdot}10^{17}$	$1{\cdot}10^{17}$